Punjab University Journal of Mathematics (2025), 57(03), 265-282
https://doi.org/10.52280/pujm.2025.57(03)02

Analytical solutions of time-fractional non-linear model Clannish Random Walker's Parabolic equation and its sensitivity

Hira Ashaq
Department of Mathematics, University of Management and Technology, Lahore, Pakistan

Muhammad Imran Asjad
Department of Mathematics, University of Management and Technology, Lahore, Pakistan
Center for Theoretical Physics, Khazar University, 41 Mehseti str., Baku, AZ1096, Azerbaijan

*Sheikh Zain Majid
Department of Mathematics, University of Management and Technology, Lahore, Pakistan

Waqas Ali Faridi
Department of Mathematics, University of Management and Technology, Lahore, Pakistan

*Corresponding Author
zain2ndaugust@gmail.com

Received:13 November, 2023 / Accepted: 03 July, 2025 / Published online: 23 September, 2025

Abstract. In this article, the exact travelling wave solutions for the non-linear time-fractional Clannish Random Walker's Parabolic equation are discussed. This study establishes the new extended direct algebraic method in which periodic, bright, multiple U-shaped bright and kink-type wave solitons are obtained with exact solutions offered by the mixed hyperbolic and trigonometry solutions, mixed periodic and periodic solutions, plane solutions, shock solutions, mixed trigonometric solutions, mixed singular solutions, mixed shock single solutions, complex solitary singular solutions, shock solutions and shock wave solutions. The obtained solutions of the non-linear time-fractional Clannish Random Walker's Parabolic equation model are graphically presented for different values of the involved parameters using `Wolfram Mathematica` software. The propagating behaviours are visualised through 3D, contour, and 2D surface plots to illustrate the influence of key parameters on the solution profiles. The time-fractional derivative introduces a memory effect into the model, making it more suitable for describing real-world physical processes that involve hereditary and nonlocal behaviour. The presence of novel soliton structures, such as multiple U-shaped solitons and bright-shaped solitons, further highlights the novelty and complexity of the model's dynamics. In this study, a planar dynamical system is constructed from the proposed model to carry out a sensitivity analysis of initial conditions. This transformation enables the investigation of how small variations in the initial values influence the system's long-term behaviour. The proposed method proves to be efficient, reliable, and broadly applicable for generating new analytical solutions to both integer and non-integer-order differential equations arising in mathematical physics and engineering.

Keywords: New extended direct algebraic method; Time-fractional Clannish Random Walker's Parabolic equation; Exact solution.

1. INTRODUCTION

The time-fractional Clannish Random Walker's Parabolic (CRWP) equation [13, 19] determine the behaviour of two Random Walker's species A and B who possess out one-dimensional and concurrent random walk characterised by a rise in the clannishness of members of the one species A at point x at time t, $U(t, x)$ can be written by the time-fractional CRWP equation as,

$$D_t^{\alpha_1} U + jU_x + kUU_x + lU_{xx} = 0, \tag{1. 1}$$

where α_1 denotes the order of the fractional time derivatives and $0 < \alpha_1 \leq 1$.
Exact solutions for travelling waves for the non-linear fractional partial differential equations (FPDEs) are important in studying physical phenomena. In recent years, partial and ordinary fractional equations have been used in modelling many chemistry, engineering, physics and biology problems [14]. In the literature, several definitions of the fractional derivatives are available, including Riemann Liouville [35, 23], the conformable fractional derivative [18, 36] and the new truncated M-fractional derivative [20]. The non-linear (PDEs) are essential for investigating the non-linear physical situation. PDEs) play an important role in many analyses because of their intermittent appearance, well-designed, and potential in various non-linear fields. To find the exact solitary wave solution in various aspects, several authors have employed different approaches [40, 38, 17, 21, 30]. The accurate and solitary wave solution of the (PDEs) was obtained by many authors using various approaches in various contexts. In both pure and applied mathematics, non-linear (PDEs) have become more significant and useful in recent years. (PDEs) They are crucial for addressing many technical and physical issues, and no one can afford to ignore them.
The travelling wave hypothesis has evolved into the primary method for analysing and extracting soliton solutions to the many non-linear evolution equations (NLEEs). Researchers have paid close attention to closed forms of exact solutions in recent years. Such solutions are critical in studying the stability and nature of physical systems. The bell and kink-shaped solitons are commonly used to simulate the non-linear oscillatory events in plasma, hydrodynamics and fibre optics. In recent years, various types of closed-form solutions of NLEEs, such as soliton, rational, coupon, periodic and quasi-periodic solutions, have been reported. Non-linear PDEs have a very vast range of practical applications in the field of wave theory, including transportation of heat and mass, plasma physics and hydrodynamics chemical technology [26, 34], ocean waves process may be characterized by non-linear ordinary differential equation systems [27], population ecology [15], electromagnetic wave interaction in a plasma [44], non-linear may appear in quantum mechanics in several different ways [8, 6] and so on.
The soliton begins with John Scott Russell's observation of the translation wave. Before Russell's work was proven in the 1870s, prominent philosophers and scientists widely praised its scientific implications. Nonetheless, Rayleigh and Boussinesq's work demonstrates the critical issue of non-linearity and dispersion. It is still rendering to address Stokes and Airy's argument against using kink-shaped and bell-shaped solutions to simulate wave phenomena in the optical fibre, the elastic media and other important fields, well-known examples include the travelling wave solutions of Korteweg de Vries and the Boussinesq equation [16, 28, 31, 32].
There are multiple approaches and schemes such as the sine-Gordon expansion scheme

[11], the Kudryashov method [41], the simply extended equation method [24] and the bilinear neural network technique [43], used to obtain exact soliton solutions for non-linear partial differential equations, [22] variational iteration method [37], extended exponential function method [25], Hirota bilinear technique [3], power series method [12], F-expansion technique [42] as well as several others [29, 2, 7, 5, 4, 1].
In the literature, there are a few approaches that are commonly used for obtaining exact solutions to the integrable wave Eq. (1), adapted (G^2/G)-expansion scheme [9] and modified extended auxiliary equation mapping [33]. The proposed method is more reliable, computationally efficient, and useful for extracting dark, bright, and singular solitons than the current analytical method.
To our knowledge, the time-fractional CRWP equation model has not yet been studied using the new extended direct algebraic method. As a result, the new extended direct algebraic method approach is used to find stable soliton solutions to non-linear (FPDE), especially the time-fractional CRWP equation also sensitive analysis is ignored in previous studies. The present methodology has some advantages over the previously studied techniques in the form of a more generalised solution, and its performance is more efficient and effective. The solitonic patterns of the time-fractional CRWP equation have been illustrated via exact solutions offered by travelling wave solutions obtained, including periodic and singular waves, multiple U-shaped bright and kink-type wave solutions by using a new extended direct algebraic method. The obtained solutions are represented as mixed hyperbolic and trigonometric solutions, periodic and mixed periodic solutions, plane solutions, shock solutions, mixed trigonometric solutions, mixed singular solutions, mixed shock single solutions, complex solitary singular solutions, and shock solutions. Comparisons are provided diagrammatically for generalised time-fractional CRWP equation solutions, represented graphically in Mathematica by varying the embedded parameter values. The applicability of the obtained typical solitary wave solutions of the considered model has been investigated here by drawing 3-D, contour and 2-D graphs of the obtained solitons. The New Extended Direct Algebraic Method is powerful for constructing exact solutions, it is limited by the form of the equation, the need for simplification, and its inability to automatically address broader physical interpretation, stability, or generality. We hope our findings will help physicists predict new ideas in mathematical physics and its applications.
In section 2, we used the new extended direct algebraic method to develop exact solutions. Section 3 demonstrates the application of the proposed method. In section 4, we observed different wave appearances in the 3-D, contour and 2-D graphical representations of the soliton solutions for different values of the wave velocity and discussed the graphical presentation of research findings with comparative analysis. Section 5 demonstrates a sensitive assessment of the considered model. Section 6 contains the conclusion of our proposed study.

2. Description of method

2.1. **Illustration of proposed method.** Consider the general (NPDE):

$$X(U, U_t, U_x, U_{tt}, U_{xx}, ...) = 0. \tag{2. 2}$$

Eq. (2. 2) can be transformed into ODE of the form given in Eq. (2. 3),

$$Y(N, N', N'', ...) = 0, \tag{2. 3}$$

this result can be achieved by using the approperiate transform given in Eq. (2. 4),

$$U(x,t) = N(\zeta), \tag{2. 4}$$

where $\zeta = k_1 x + k_2 t$ and k_1, k_2 are real constants. Assume $N(\zeta)$ in the solution of Eq. (2. 3) and can be written in the series form as follows:

$$N(\zeta) = a_0 + \sum_{i=1}^{M} [a_i(\mathfrak{F}(\zeta))^i], \tag{2. 5}$$

where,

$$\mathfrak{F}'(\zeta) = \ln(A)(\wp + \mathfrak{B}\mathfrak{F}(\zeta) + \lambda\mathfrak{F}^2(\zeta)),\ A \neq 0, 1, \tag{2. 6}$$

where, $\wp, \mathfrak{B}$ and λ are real constants and $S = \mathfrak{B}^2 - 4\wp\lambda$. The general solutions with respect to parameters $\wp, \mathfrak{B}$ and λ of Eq. (2. 6) are:

(Case 1): When $\mathfrak{B}^2 - 4\wp\lambda < 0$ and $\lambda \neq 0$,

$$\mathfrak{F}_1(\zeta) = -\frac{\mathfrak{B}}{2\lambda} + \frac{\sqrt{-S}}{2\lambda}\tan_A(\frac{\sqrt{-S}}{2}\zeta), \tag{2. 7}$$

$$\mathfrak{F}_2(\zeta) = -\frac{\mathfrak{B}}{2\lambda} - \frac{\sqrt{-S}}{2\lambda}\cot_A(\frac{\sqrt{-S}}{2}\zeta), \tag{2. 8}$$

$$\mathfrak{F}_3(\zeta) = -\frac{\mathfrak{B}}{2\lambda} + \frac{\sqrt{-S}}{2\lambda}(\tan_A(\sqrt{-S}\zeta) \pm \sqrt{uv}\sec_A(\sqrt{-S}\zeta)), \tag{2. 9}$$

$$\mathfrak{F}_4(\zeta) = -\frac{\mathfrak{B}}{2\lambda} + \frac{\sqrt{-S}}{2\lambda}(\cot_A(\sqrt{-S}\zeta) \pm \sqrt{uv}\csc_A(\sqrt{-S}\zeta)), \tag{2. 10}$$

$$\mathfrak{F}_5(\zeta) = -\frac{\mathfrak{B}}{2\lambda} + \frac{\sqrt{-S}}{4\lambda}(\tan_A(\frac{\sqrt{-S}}{4}\zeta) - \cot_A(\frac{\sqrt{-S}}{4}\zeta)). \tag{2. 11}$$

(Case 2): When $\mathfrak{B}^2 - 4\wp\lambda > 0$ and $\lambda \neq 0$,

$$\mathfrak{F}_6(\zeta) = -\frac{\mathfrak{B}}{2\lambda} - \frac{\sqrt{S}}{2\lambda}\tanh_A(\frac{\sqrt{S}}{2}\zeta), \tag{2. 12}$$

$$\mathfrak{F}_7(\zeta) = -\frac{\mathfrak{B}}{2\lambda} - \frac{\sqrt{S}}{2\lambda}\coth_A(\frac{\sqrt{S}}{2}\zeta), \tag{2. 13}$$

$$\mathfrak{F}_8(\zeta) = -\frac{\mathfrak{B}}{2\lambda} + \frac{\sqrt{S}}{2\lambda}(-\tanh_A(\sqrt{S}\zeta) \pm \iota\sqrt{uv}\,\mathrm{sech}_A(\sqrt{S}\zeta)), \tag{2. 14}$$

$$\mathfrak{F}_9(\zeta) = -\frac{\mathfrak{B}}{2\lambda} + \frac{\sqrt{S}}{2\lambda}(-\coth_A(\sqrt{S}\zeta) \pm \sqrt{uv}\,\mathrm{csch}_A(\sqrt{S}\zeta)), \tag{2. 15}$$

$$\mathfrak{F}_{10}(\zeta) = -\frac{\mathfrak{B}}{2\lambda} - \frac{\sqrt{S}}{4\lambda}(\tanh_A(\frac{\sqrt{S}}{4}\zeta) + \coth_A(\frac{\sqrt{S}}{4}\zeta)). \tag{2. 16}$$

(Case 3): When $\wp\lambda > 0$ and $\mathfrak{B} = 0$,

$$\mathfrak{F}_{11}(\zeta) = \sqrt{\frac{\wp}{\lambda}}\tan_A(\sqrt{\wp\lambda}\zeta), \tag{2. 17}$$

$$\mathfrak{F}_{12}(\zeta) = -\sqrt{\frac{\wp}{\lambda}}\cot_A(\sqrt{\wp\lambda}\zeta), \tag{2. 18}$$

$$\mathfrak{F}_{13}(\zeta)=\sqrt{\frac{\wp}{\lambda}}(\tan_A(2\sqrt{\wp\lambda}\zeta)\pm\sqrt{uv}\sec_A(2\sqrt{\wp\lambda}\zeta)), \tag{2. 19}$$

$$\mathfrak{F}_{14}(\zeta)=\sqrt{\frac{\wp}{\lambda}}(-\cot_A(2\sqrt{\wp\lambda}\zeta)\pm\sqrt{uv}\csc_A(2\sqrt{\wp\lambda}\zeta)), \tag{2. 20}$$

$$\mathfrak{F}_{15}(\zeta)=\frac{1}{2}\sqrt{\frac{\wp}{\lambda}}(\tan_A(\frac{\sqrt{\wp\lambda}}{2}\zeta)-\cot_A(\frac{\sqrt{\wp\lambda}}{2}\zeta)). \tag{2. 21}$$

(Case 4): When $\wp\lambda<0$ and $\mathfrak{B}=0$,

$$\mathfrak{F}_{16}(\zeta)=-\sqrt{-\frac{\wp}{\lambda}}\tanh_A(\sqrt{-\wp\lambda}\zeta), \tag{2. 22}$$

$$\mathfrak{F}_{17}(\zeta)=-\sqrt{-\frac{\wp}{\lambda}}\coth_A(\sqrt{-\wp\lambda}\zeta), \tag{2. 23}$$

$$\mathfrak{F}_{18}(\zeta)=\sqrt{-\frac{\wp}{\lambda}}(-\tanh_A(2\sqrt{-\wp\lambda}\zeta)\pm\iota\sqrt{uv}\,\mathrm{sech}_A(2\sqrt{-\wp\lambda}\zeta)), \tag{2. 24}$$

$$\mathfrak{F}_{19}(\zeta)=\sqrt{-\frac{\wp}{\lambda}}(-\coth_A(2\sqrt{-\wp\lambda}\zeta)\pm\sqrt{uv}\,\mathrm{csch}_A(2\sqrt{-\wp\lambda}\zeta)), \tag{2. 25}$$

$$\mathfrak{F}_{20}(\zeta)=-\frac{1}{2}\sqrt{-\frac{\wp}{\lambda}}(\tanh_A(\frac{\sqrt{-\wp\lambda}}{2}\zeta)+\coth_A(\frac{\sqrt{-\wp\lambda}}{2}\zeta)). \tag{2. 26}$$

(Case 5): When $\mathfrak{B}=0$ and $\wp=\lambda$,

$$\mathfrak{F}_{21}(\zeta)=\tan_A(\wp\zeta), \tag{2. 27}$$

$$\mathfrak{F}_{22}(\zeta)=-\cot_A(\wp\zeta), \tag{2. 28}$$

$$\mathfrak{F}_{23}(\zeta)=\tan_A(2\wp\zeta)\pm\sqrt{uv}\sec_A(2\wp\zeta), \tag{2. 29}$$

$$\mathfrak{F}_{24}(\zeta)=-\cot_A(2\wp\zeta)\pm\sqrt{uv}\csc_A(2\wp\zeta), \tag{2. 30}$$

$$\mathfrak{F}_{25}(\zeta)=\frac{1}{2}(\tan_A(\frac{\wp}{2}\zeta)-\cot_A(\frac{\wp}{2}\zeta)). \tag{2. 31}$$

(Case 6): When $\mathfrak{B}=0$ and $\wp=-\lambda$,

$$\mathfrak{F}_{26}(\zeta)=-\tanh_A(\wp\zeta), \tag{2. 32}$$

$$\mathfrak{F}_{27}(\zeta)=-\coth_A(\wp\zeta), \tag{2. 33}$$

$$\mathfrak{F}_{28}(\zeta)=-\tanh_A(2\wp\zeta)\pm\iota\sqrt{uv}\,\mathrm{sech}_A(2\wp\zeta), \tag{2. 34}$$

$$\mathfrak{F}_{29}(\zeta)=-\cot_A(2\wp\zeta)\pm\sqrt{uv}\,\mathrm{csch}_A(2\wp\zeta), \tag{2. 35}$$

$$\mathfrak{F}_{30}(\zeta)=-\frac{1}{2}(\tanh_A(\frac{\wp}{2}\zeta)+\cot_A(\frac{\wp}{2}\zeta)). \tag{2. 36}$$

(Case 7): When $\mathfrak{B}^2=4\wp\lambda$,

$$\mathfrak{F}_{31}(\zeta)=\frac{-2\wp(\mathfrak{B}\zeta\ln(A)+2)}{\mathfrak{B}^2\zeta\ln(A)}. \tag{2. 37}$$

(Case 8): When $\mathfrak{B}=p$, $\wp=pq$, $(q\neq 0)$ and $\lambda=0$,

$$\mathfrak{F}_{32}(\zeta)=A^{p\zeta}-q. \tag{2. 38}$$

(Case 9): When $\mathfrak{B}=\lambda=0$,

$$\mathfrak{F}_{33}(\zeta)=\wp\zeta\ln(A). \tag{2. 39}$$

(Case 10): When $\wp = \mathfrak{B} = 0$,

$$\mathfrak{F}_{34}(\zeta) = \frac{-1}{\lambda\zeta\ln(A)}. \tag{2. 40}$$

(Case 11): When $\wp = 0$, and $\mathfrak{B} \neq 0$,

$$\mathfrak{F}_{35}(\zeta) = -\frac{u\mathfrak{B}}{\lambda(\cosh_A(\mathfrak{B}\zeta) - \sinh_A(\mathfrak{B}\zeta) + u)}, \tag{2. 41}$$

$$\mathfrak{F}_{36}(\zeta) = -\frac{\mathfrak{B}(\sinh_A(\mathfrak{B}\zeta) + \cosh_A(\mathfrak{B}\zeta))}{\lambda(\sinh_A(\mathfrak{B}\zeta) + \cosh_A(\mathfrak{B}\zeta) + v)}. \tag{2. 42}$$

(Case 12): When $\mathfrak{B} = p$, $\lambda = pq$, $(q \neq 0)$ and $\wp = 0$,

$$\mathfrak{F}_{37}(\zeta) = -\frac{uA^{p\zeta}}{u - qvA^{p\zeta}}. \tag{2. 43}$$

$$\begin{aligned}
&\sinh_A(\zeta) = \frac{uA^{\zeta} - vA^{-\zeta}}{2}\ ,\ \cosh_A(\zeta) = \frac{uA^{\zeta} + vA^{-\zeta}}{2},\\
&\tanh_A(\zeta) = \frac{uA^{\zeta} - vA^{-\zeta}}{uA^{\zeta} + vA^{-\zeta}}\ ,\ \coth_A(\zeta) = \frac{uA^{\zeta} + vA^{-\zeta}}{uA^{\zeta} - vA^{-\zeta}},\\
&\operatorname{sech}_A(\zeta) = \frac{2}{uA^{\zeta} + vA^{-\zeta}}\ ,\ \operatorname{csch}_A(\zeta) = \frac{2}{uA^{\zeta} - vA^{-\zeta}},\\
&\sin_A(\zeta) = \frac{uA^{\iota\zeta} - vA^{-\iota\zeta}}{2\iota}\ ,\ \cos_A(\zeta) = \frac{uA^{\iota\zeta} + vA^{-\iota\zeta}}{2},\\
&\tan_A(\zeta) = -\iota\frac{uA^{\iota\zeta} - vA^{-\iota\zeta}}{uA^{\iota\zeta} + vA^{-\iota\zeta}}\ ,\ \cot_A(\zeta) = \iota\frac{uA^{\iota\zeta} + vA^{-\iota\zeta}}{uA^{\iota\zeta} - vA^{-\iota\zeta}},\\
&\sec_A(\zeta) = \frac{2}{uA^{\zeta} + vA^{-\zeta}}\ ,\ \csc_A(\zeta) = \frac{2\iota}{uA^{\zeta} - vA^{-\zeta}}.
\end{aligned} \tag{2. 44}$$

The deformation arbitrary constants parameters u and v are greater than zero.

3. Exact solutions for CRWP equation

We use the following travelling wave to obtain the solutions of Eq. (1. 1), transformation:

$$\mathfrak{U}(x,t) = \mathfrak{U}(\zeta) \textit{ where } \zeta = x - \frac{c}{\Omega}\left(t + \frac{1}{\lambda(\Omega)}\right)^{\Omega}, \tag{3. 45}$$

where c is constant. On the contrivance of Eq. (3. 45) to the Eq. (1. 1), we reveal that:

$$2(j-c)N + kN^2 + 2lN' = 0. \tag{3. 46}$$

According to the homogeneous balancing principle of Eq. (3. 46) gives $M = 1$.

$$\mathfrak{U}(x,t) = a_0 + a_1\mathfrak{F}(\zeta), \tag{3. 47}$$

where,

$$\mathfrak{F}'(\zeta) = \ln(A)(\wp + \mathfrak{B}\mathfrak{F}(\zeta) + \lambda\mathfrak{F}^2(\zeta)),\ A \neq 0, 1, \tag{3. 48}$$

The prognosticate solution Eq. (3. 47) is plugging in Eq. (3. 46) and equating the coefficient of distinct power of $\mathfrak{F}(\zeta)$ prevailed the algebraic system of equations:

$$\begin{aligned}(\mathfrak{F}(\zeta))^0 &: 2ja_0 - 2ca_0 + ka_0^2 + 2la_1\ln(A)\wp,\\ (\mathfrak{F}(\zeta))^1 &: 2ja_1 - 2ca_1 + 2ka_0a_1 + 2la_1\ln(A)\mathfrak{B},\\ (\mathfrak{F}(\zeta))^2 &: ka_1^2 + 2la_1\ln(A)\lambda.\end{aligned} \tag{3. 49}$$

system of Eq. (3. 49) is solved with the help of the modern software `Mathematica` to get the required parameters,

$$a_0 = \frac{l\ln(A)}{k}(\mathfrak{B} \pm \sqrt{S}),\ a_1 = \frac{2l\ln(A)}{k}\lambda,\ c = j + \ln(A)(\mathfrak{B}l - \mathfrak{B} \pm l\sqrt{S}). \tag{3. 50}$$

$$\mathfrak{U}(x,t) = \Pi\mathfrak{B} \pm \Pi\sqrt{S} + 2\Pi\lambda[\mathfrak{F}_i(\zeta)]. \tag{3. 51}$$

Where, $\Pi = \frac{\ln(A)l}{k}$ and $S = \mathfrak{B}^2 - 4\wp\lambda$.
Exact solutions for Eq. (1. 1) can be obtained by plugging the Eq. (3. 50) into Eq. (3. 47), which is given below,
(Case 1): When $\mathfrak{B}^2 - 4\wp\lambda < 0$ and $\lambda \neq 0$,

$$\mathfrak{U}_1(x,t) = \Pi\sqrt{S}(1 + \iota\tan_A(\frac{\sqrt{-S}}{2}\zeta)), \tag{3. 52}$$

$$\mathfrak{U}_2(x,t) = \Pi\sqrt{S}(1 - \iota\cot_A(\frac{\sqrt{S}}{2}\zeta)), \tag{3. 53}$$

$$\mathfrak{U}_3(x,t) = \Pi\sqrt{S}(1 + \iota(\tan_A(\sqrt{-S}\zeta) \pm \sqrt{uv}\sec_A(\sqrt{-S}\zeta))), \tag{3. 54}$$

$$\mathfrak{U}_4(x,t) = \Pi\sqrt{S}(1 + \iota(\cot_A(\sqrt{-S}\zeta) \pm \sqrt{uv}\csc_A(\sqrt{-S}\zeta))), \tag{3. 55}$$

$$\mathfrak{U}_5(x,t) = \Pi\sqrt{S}(1 + \frac{\iota}{2}(\tan_A(\frac{\sqrt{-S}}{4}\zeta) - \cot_A(\frac{\sqrt{-S}}{4}\zeta))). \tag{3. 56}$$

(Case 2): When $\mathfrak{B}^2 - 4\wp\lambda > 0$ and $\lambda \neq 0$,

$$\mathfrak{U}_6(x,t) = \Pi\sqrt{S}(1 - \tan_A(\frac{\sqrt{S}}{2}\zeta)), \tag{3. 57}$$

$$\mathfrak{U}_7(x,t) = \Pi\sqrt{S}(1 - \cot_A(\frac{\sqrt{S}}{2}\zeta)), \tag{3. 58}$$

$$\mathfrak{U}_8(x,t) = \Pi\sqrt{S}(1 - \tan_A(\sqrt{S}\zeta) \pm \iota\sqrt{uv}\sec_A(\sqrt{S}\zeta))), \tag{3. 59}$$

$$\mathfrak{U}_9(x,t) = \Pi\sqrt{S}(1 - \cot_A(\sqrt{S}\zeta) \pm \sqrt{uv}\csc_A(\sqrt{S}\zeta))), \tag{3. 60}$$

$$\mathfrak{U}_{10}(x,t) = \Pi\sqrt{S}(1 + \frac{1}{2}(\tan_A(\frac{\sqrt{S}}{4}\zeta) + \cot_A(\frac{\sqrt{S}}{4}\zeta))). \tag{3. 61}$$

(Case 3): When $\wp\lambda > 0$ and $\mathfrak{B} = 0$,

$$\mathfrak{U}_{11}(x,t) = 2\Pi\sqrt{\lambda}(\sqrt{\wp}\tan_A(\sqrt{\wp\lambda}\zeta + \sqrt{\wp}\iota), \tag{3. 62}$$

$$\mathfrak{U}_{12}(x,t) = 2\Pi\sqrt{\lambda}(-\sqrt{\wp}\cot_A(\sqrt{\wp\lambda}\zeta + \sqrt{\wp}\iota), \tag{3. 63}$$

$$\mathfrak{U}_{13}(x,t) = 2\Pi\sqrt{\lambda}(\sqrt{\wp}(\tan_A(2\sqrt{\wp\lambda}\zeta) \pm \sqrt{uv}\sec_A(2\sqrt{\wp\lambda}\zeta)) + \sqrt{\wp}\iota), \tag{3. 64}$$

$$\mathfrak{U}_{14}(x,t) = 2\Pi\sqrt{\lambda}(\sqrt{\wp}(-\cot_A(2\sqrt{\wp\lambda}\zeta) \pm \sqrt{uv}\csc_A(2\sqrt{\wp\lambda}\zeta)) + \sqrt{\wp}\iota), \tag{3. 65}$$

$$\mathfrak{U}_{15}(x,t) = 2\Pi\sqrt{\lambda}(\frac{\sqrt{\wp}}{2}(\tan_A(\frac{\sqrt{\wp\lambda}}{2}\zeta - \cot_A(\frac{\sqrt{\wp\lambda}}{2}\zeta)) + \sqrt{\wp}\iota). \tag{3. 66}$$

(Case 4): When $\wp\lambda < 0$ and $\mathfrak{B} = 0$,

$$\mathfrak{U}_{16}(x,t) = 2\Pi\sqrt{\lambda}(-\sqrt{-\wp}\tanh_A(\sqrt{-\wp\lambda}\zeta) + \sqrt{\wp}\iota), \tag{3. 67}$$

$$\mathfrak{U}_{17}(x,t) = 2\Pi\sqrt{\lambda}(-\sqrt{-\wp}\coth_A(\sqrt{-\wp\lambda}\zeta) + \sqrt{\wp}\iota), \tag{3. 68}$$

$$\mathfrak{U}_{18}(x,t) = 2\Pi\sqrt{\lambda}(\sqrt{-\wp}(-\tanh_A(2\sqrt{-\wp\lambda}\zeta) \pm \iota\sqrt{uv}\,\mathrm{sech}_A(2\sqrt{-\wp\lambda}\zeta)) + \sqrt{\wp}\iota), \tag{3. 69}$$

$$\mathfrak{U}_{19}(x,t) = 2\Pi\sqrt{\lambda}(\sqrt{-\wp}(-\coth_A(2\sqrt{-\wp\lambda}\zeta \pm \sqrt{uv}\,\mathrm{csch}_A(2\sqrt{-\wp\lambda}\zeta)) + \sqrt{\wp}\iota), \tag{3. 70}$$

$$\mathfrak{U}_{20}(x,t) = 2\Pi\sqrt{\lambda}(-\frac{\sqrt{-\wp}}{2}(\tanh_A(\frac{\sqrt{-\wp\lambda}}{2}\zeta) + \coth(\frac{\sqrt{-\wp\lambda}}{+}\sqrt{\wp}\iota). \tag{3. 71}$$

(Case 5): When $\mathfrak{B} = 0$ and $\wp = \lambda$,

$$\mathfrak{U}_{21}(x,t) = 2\Pi\wp(\tan_A(\wp\zeta) + \iota), \tag{3. 72}$$

$$\mathfrak{U}_{22}(x,t) = 2\Pi\wp(-\cot_A(\wp\zeta) + \iota), \tag{3. 73}$$

$$\mathfrak{U}_{23}(x,t) = 2\Pi\wp(\tan_A(2\wp\zeta) \pm \sqrt{uv}\sec_A(2\wp\zeta) + \iota), \tag{3. 74}$$

$$\mathfrak{U}_{24}(x,t) = 2\Pi\wp(-\cot_A(2\wp\zeta) \pm \sqrt{uv}\csc_A(2\wp\zeta) + \iota), \tag{3. 75}$$

$$\mathfrak{U}_{25}(x,t) = 2\Pi\wp(\frac{1}{2}\tan_A(\frac{\wp}{2}\zeta) - \cot_A(\frac{\wp}{2}\zeta) + \iota). \tag{3. 76}$$

(Case 6): When $\mathfrak{B} = 0$ and $\lambda = -\wp$,

$$\mathfrak{U}_{26}(x,t) = 2\Pi\wp(1 + \tanh_A(\wp\zeta)), \tag{3. 77}$$

$$\mathfrak{U}_{27}(x,t) = 2\Pi\wp(1 + \coth_A(\wp\zeta)), \tag{3. 78}$$

$$\mathfrak{U}_{28}(x,t) = 2\Pi\wp(1 + \tanh_A(2\wp\zeta) \mp \iota\sqrt{uv}\sec_A(2\wp\zeta)), \tag{3. 79}$$

$$\mathfrak{U}_{29}(x,t) = 2\Pi\,\wp(1 + \cot_A(2\,\wp\,\zeta) \mp \sqrt{uv}\,\mathrm{csch}_A(2\,\wp\,\zeta)), \tag{3. 80}$$

$$\mathfrak{U}_{30}(x,t) = 2\Pi\wp(1 + \frac{1}{2}(\tanh_A(\frac{\wp}{2}\zeta) - \cot_A(\frac{\wp}{2}\zeta))). \tag{3. 81}$$

(Case 7): When $\mathfrak{B}^2 = 4\wp\lambda$,

$$\mathfrak{U}_{31}(x,t) = \Pi\mathfrak{B} + 2\Pi\lambda(-\frac{2\wp(\mathfrak{B}\zeta\ln(A) + 2)}{\mathfrak{B}^2\zeta\ln(A)}. \tag{3. 82}$$

(Case 8): When $\mathfrak{B} = p$, $\wp = pq$, $(q \neq 0)$ and $\lambda = 0$,

$$\mathfrak{U}_{32}(x,t) = 2\Pi p. \tag{3. 83}$$

(Case 9): When $\mathfrak{B} = \lambda = 0$,

$$\mathfrak{U}_{33}(x,t) = 0. \tag{3. 84}$$

(Case 10): When $\wp = \mathfrak{B} = 0$,

$$\mathfrak{U}_{34}(x,t) = 2\Pi(\frac{-1}{\zeta\ln(A)}. \tag{3. 85}$$

(Case 11): When $\wp = 0$, and $\mathfrak{B} \neq 0$,

$$\mathfrak{U}_{35}(x,t) = 2\Pi(\frac{-u\wp}{\cosh_A(\wp\zeta) - \sinh_A(\wp\zeta) + u} + \iota\sqrt{\wp\lambda}), \tag{3. 86}$$

$$\mathfrak{U}_{36}(x,t) = 2\Pi(\frac{-\wp(\sinh_A(\wp\zeta) + \cosh_A(\wp\zeta)}{\sinh_A(\wp\zeta) + \cosh_A(\wp\zeta) + v} + \iota\sqrt{\wp\lambda}). \tag{3. 87}$$

(Case 12): When $\mathfrak{B} = p$, $\lambda = pq$, $(q \neq 0)$ and $\wp = 0$,

$$\mathfrak{U}_{37}(x,t) = 2\Pi p(\frac{-uA^p\zeta}{u - qvA^p\zeta} + \iota\sqrt{q}). \tag{3. 88}$$

4. Graphically Discussion

This section explains numerical and physical simulations of some obtained solutions to the successive non-linear evolution equations of the time-fractional Clannish Random Walker's Parabolic equation by selecting appropriate values for the arbitrary parameters. A modern software program, `Wolfram Mathematica`, is utilised to plot graphs for better presentation.

In Figure 1, graphs for the soliton wave number (Ω) of the obtained solution $\mathfrak{U}_1(x,t)$, at the parametric values $\wp$=0.6, $\mathfrak{B}$=0.2, λ=0.7, A = 2, l= 5, k=0.4, u=3, v=2 and c=1, for different values of wave numbers, in the form of 3-D, contour and 2-D. In Fig. (1a) at Ω=0.1, continuous bright solitonic behaviour is observed in a 3-D profile by increasing the value of wave number, we found the same behaviour in Fig. (1d) and (1g) and for more visualization, the contour was plotted and found the bright soliton in (1b), (1e), (1h), and 2-D shows the bright periodic soliton in (1c), (1f) and (1i) by increasing values of wave speed.

In Figure 2, we examine the soliton wave number (Ω) for the derived solution $\mathfrak{U}_6(x,t)$ at specific parameter values: $\wp$=0.02, $\mathfrak{B}$=5, λ=7, A=2, l=5, k=0.4, u=3, v=2, and c=1. We visualise this wave number's impact through 3-D, 2-D, and contour plots. In Fig. (1a), when Ω is set to 3.09, we observe a continuous bright solitonic behaviour in a 3-D profile. As we increase the wave number value, this behaviour persists, as shown in Figures 1d and 1g. To provide a more detailed view, we employ contour plots and find the bright soliton in Figures (1b), (1e), and (1h). The 2-D plots reveal bright periodic solitons in Figures (1c), (1f), and (1i) as we further increase the wave speed. This analysis allows us to understand how changes in the wave number affect the behaviour of the derived solution $\mathfrak{U}_6(x,t)$ at the specified parameter values.

In Figure 3, graphs for the soliton velocity of the obtained solutions $\mathfrak{U}_{25}(x,t)$, at the parametric values $\wp$= 5, $\mathfrak{B}$= 0, λ= 5, $A = 3$, $l = 5$, $k = 0.4$, $u = 2.9$, $v = 6$, $c = 0.9$, for different values of wave number, in the form of 3-D, 2-D and contour, multiple bright solitonic behaviours are observed in 3-D, bright solitons in contour and multiple bright singular solitons can be seen in 2-D for the same values of wave number as we took in Fig.1).

In Figure 4, graphs for $\mathfrak{U}_{28}(x,t)$ for parametric values $\wp$=5, $\mathfrak{B}$=0, λ=-5, $A = 2$, $l = 5$, $k = 0.4$, $u = 3$, $v = 2$, $c = 1$ at wave speed Ω=0.1, shows flat anti-kink structure in 3-D, contour and 2-D getting bright by increasing the value of the soliton wave number.

Moreover, it is expected that future research on non-linear wave phenomena will further clarify the challenges addressed in applied sciences through the results and explanations presented in this study. The novel solutions obtained in this work can contribute to practical applications in areas such as fluid dynamics, non-linear optics, plasma physics, and biological wave propagation, where understanding and controlling wave behaviour is of critical importance.

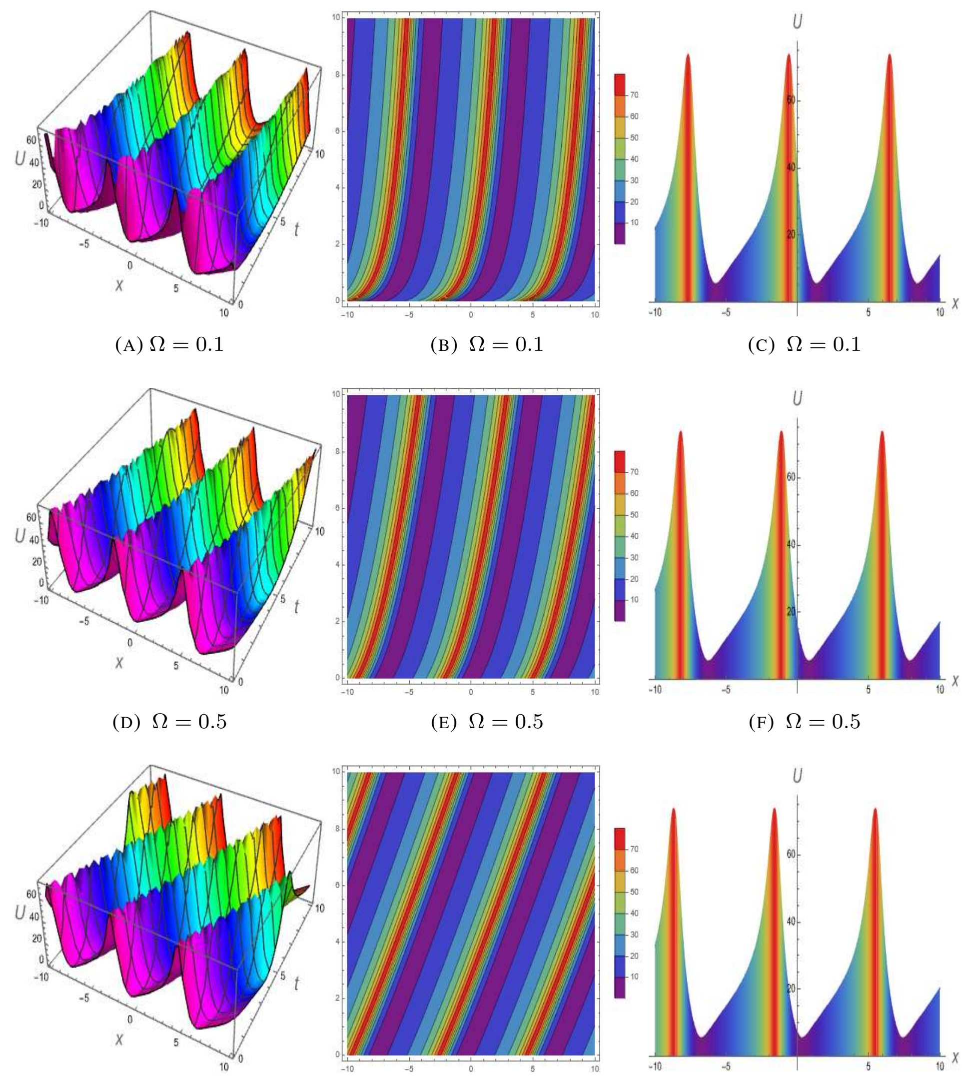

(A) $\Omega = 0.1$ (B) $\Omega = 0.1$ (C) $\Omega = 0.1$

(D) $\Omega = 0.5$ (E) $\Omega = 0.5$ (F) $\Omega = 0.5$

(G) $\Omega = 0.9$ (H) $\Omega = 0.9$ (I) $\Omega = 0.9$

FIGURE 1. Visualised impact of travelling wave velocity in 3-D, contour and 2-D for solution $\mathfrak{U}_1(x,t)$

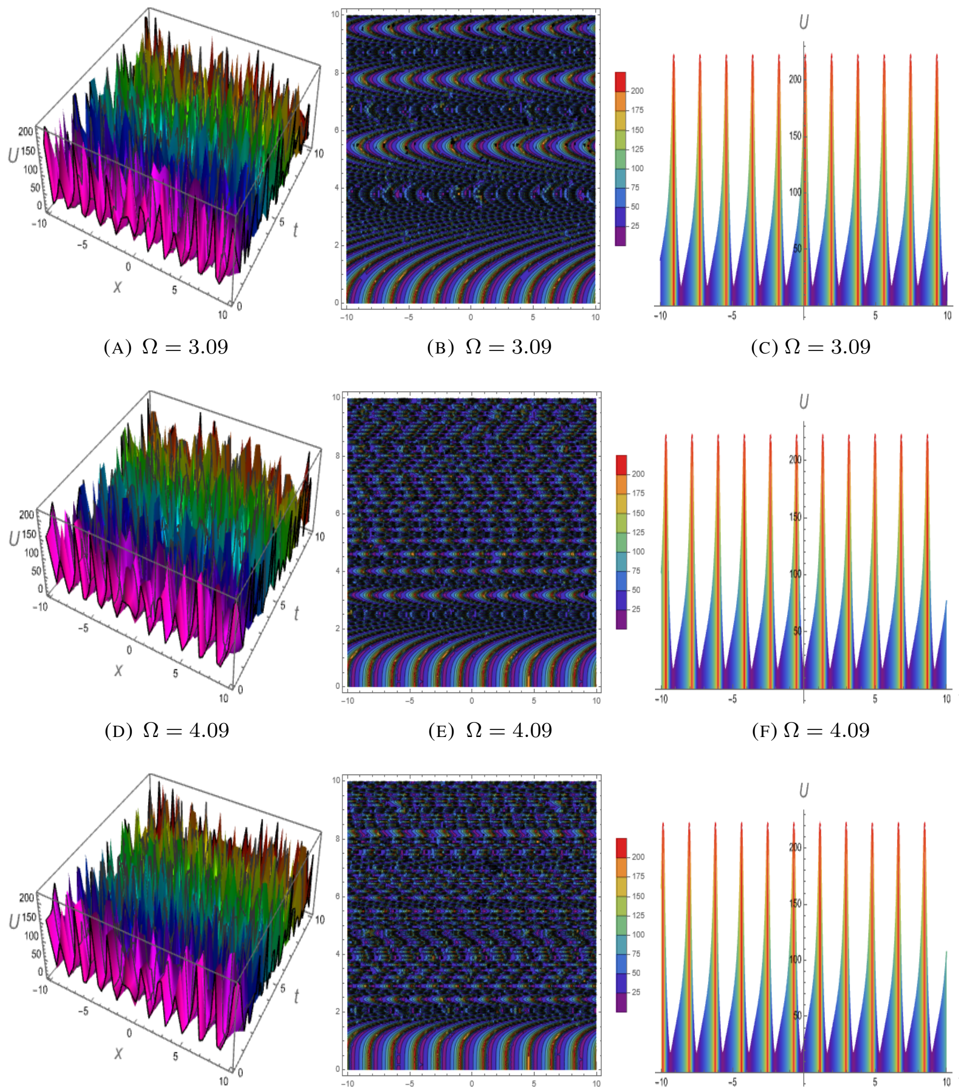

(A) $\Omega = 3.09$ (B) $\Omega = 3.09$ (C) $\Omega = 3.09$

(D) $\Omega = 4.09$ (E) $\Omega = 4.09$ (F) $\Omega = 4.09$

(G) $\Omega = 5.09$ (H) $\Omega = 5.09$ (I) $\Omega = 5.09$

FIGURE 2. Visualised impact of travelling wave velocity in 3-D, contour and 2-D for solution $\mathfrak{U}_6(x,t)$

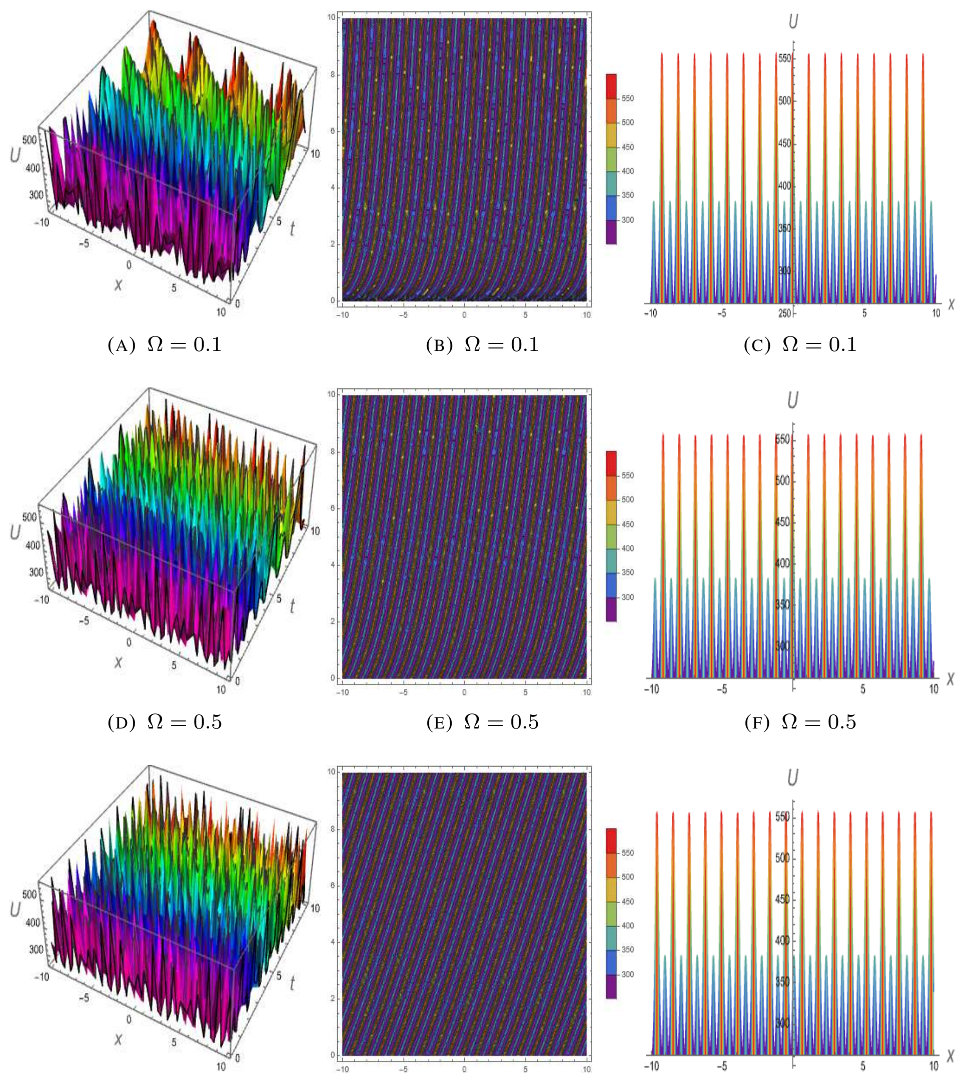

(A) $\Omega = 0.1$ (B) $\Omega = 0.1$ (C) $\Omega = 0.1$

(D) $\Omega = 0.5$ (E) $\Omega = 0.5$ (F) $\Omega = 0.5$

(G) $\Omega = 0.9$ (H) $\Omega = 0.9$ (I) $\Omega = 0.9$

FIGURE 3. Visualised impact of travelling wave velocity in 3-D, contour and 2-D for solution $\mathfrak{U}_{25}(x,t)$

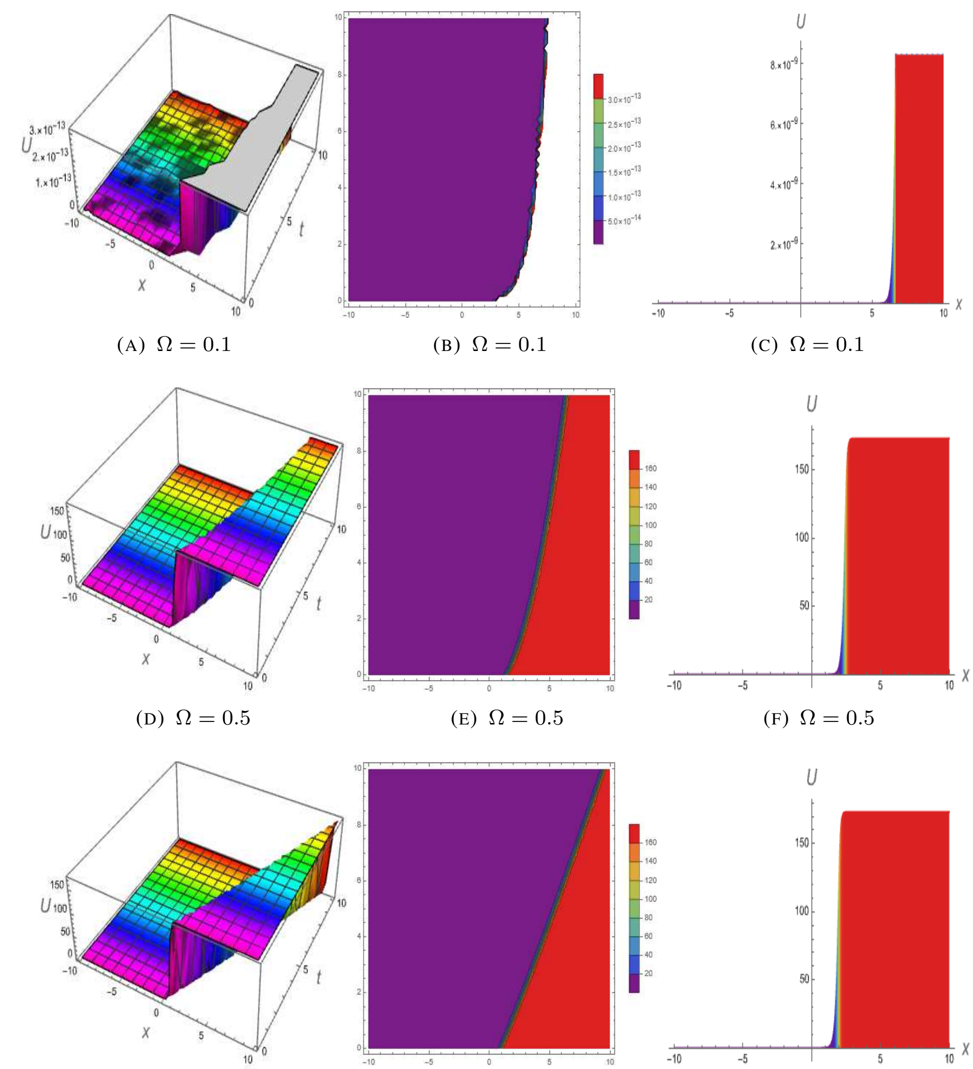

(A) $\Omega = 0.1$ (B) $\Omega = 0.1$ (C) $\Omega = 0.1$

(D) $\Omega = 0.5$ (E) $\Omega = 0.5$ (F) $\Omega = 0.5$

(G) $\Omega = 0.9$ (H) $\Omega = 0.9$ (I) $\Omega = 0.9$

FIGURE 4. Visualised impact of travelling wave velocity in 3-D, 2-D and Contour for soliton solution $\mathfrak{U}_{28}(x,t)$

4.1. **Comparison with Existing Study.** To highlight the uniqueness of this work, a comparison with existing literature is presented. Seadawy et al. [33] obtained singular, periodic, and bright solitons using the modified auxiliary and F-expansion method. Alam et al. [10] identified singular, bell-shaped, and bright solitons via the (ψ, ϕ)-expansion technique. Ullah et al. [39] reported a range of soliton types-bright, dark, singular, and combo

forms-using the extended direct algebraic method.
In contrast, the current study reveals new types of soliton solutions, including kink solitons, bright solitons, and multiple U-shaped bright solitons, along with periodic forms. This diversity of solutions, some aligning with past findings and others entirely novel, underscores the originality of the work. The applied methods proved effective in generating a wide variety of solution structures.
In addition, a sensitivity analysis has been included to explore the dynamic behaviour of the model, offering deeper insight into how small changes in initial conditions affect the system.
Physically, the solutions represent realistic wave behaviours in non-linear media: U-shaped solitons correspond to stable, localised waveforms; bright-shaped solitons illustrate regions of high intensity; and multiple U-shaped solitons capture complex, multi-peak structures. These patterns reflect wave dynamics commonly observed in real-world systems such as fluid flow, optical fibres, and other non-linear dispersive media.

5. THE SENSITIVITY ASSESSMENT

The plane dynamic system can contribute to the sensitivity of the time-fractional Clannish Random Walkers Parabolic equation. The dynamic system of Eq. (3. 46) is as follows:

$$N^{'} = \frac{-2(j-c)\,N}{2l} - \frac{k\,N^2}{2l} = 0. \tag{5. 89}$$

This section discusses the sensitive behaviour of the considered model with parametric values $c = 1.2$, $k = 0.9$, $j = 1.5$ and $l = 0.5$, after transforming it into a dynamical system (5. 89). The sensitivity of the dynamical system depends on the initial guess. By choosing a suitable initial guess, the sensitivity of the system can be controlled. If a minor adjustment in the initial conditions results in a slight change in the system, the system is less sensitive. We will establish the physical properties of the considered model and discuss the effects of the frequency and perturbation force. As a result, by using different initial conditions in the segment, we recognise the sensitivity of the solution of the dynamical system.
In Fig. (4), the main objective of the present investigation is to accurately assess the disturbance caused by the changes in the input. The analysis findings show different parametric values to illustrate how small changes in input can result in large variances in the result. In Fig. (4a), it can be illustrated that a slight change in the initial condition affects the solutions that contribute to the disorderly behaviour of the curve. The same experiment is replicated in Figs. (4b), (4c) and (6d), by retaining the values of the parameters and making a larger change in the initial conditions, and the same effects are observed; as a result, in this case, the system is sensitive.

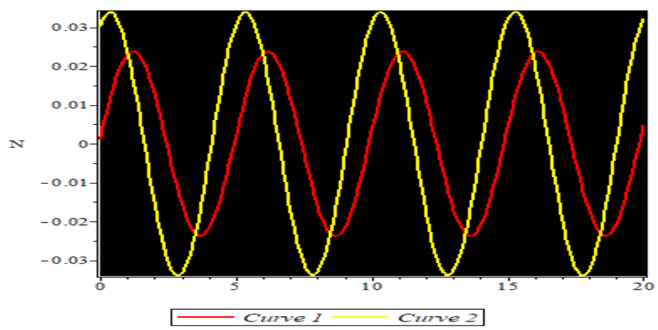

(A) Sensitive analysis for the curve 1 and curve 2 at $(0.001, 0.03)$ and $(0.03, 0.02)$ respectively.

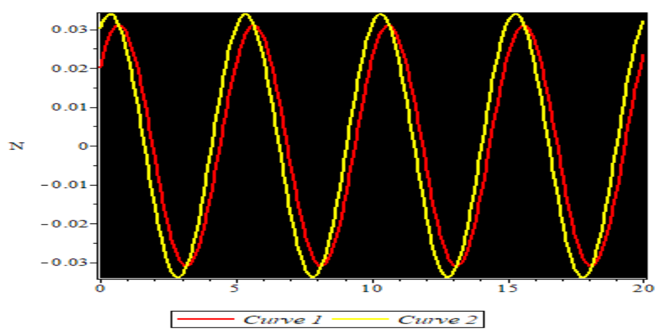

(B) Sensitive analysis for the curve 1 and cu rve 2 at $(0.02, 0.03)$ and $(0.03, 0.02)$ respectively.

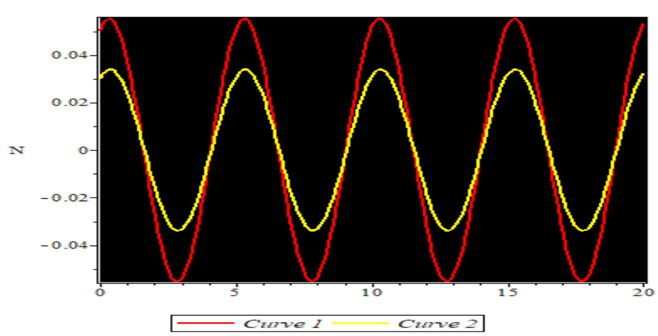

(C) Sensitive analysis for the curve the 1 and curve 2 at $(0.05, 0.03)$ and $(0.03, 0.02)$ respectively.

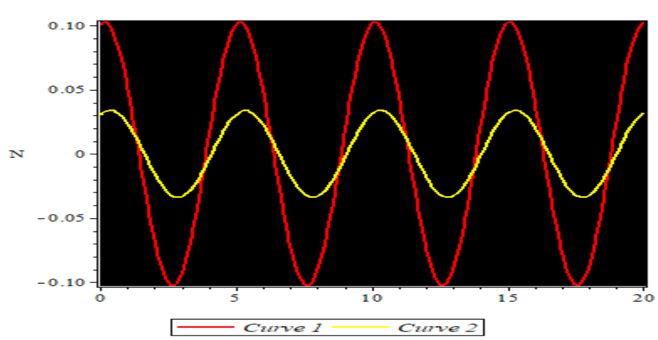

(D) Sensitive analysis for the curve 1 and curve 2, at $(0.1, 0.03)$ and $(0.03, 0.02)$ respectively.

FIGURE 5. Sensitivity visualisation at distinct initial conditions

6. CONCLUSIONS

This work explored the non-linear time-fractional Clannish Random Walker's Parabolic equation using the new extended direct algebraic method. The incorporation of time-fractional derivatives introduces memory and nonlocal effects, making the model more realistic for describing complex physical phenomena. By selecting specific parameter values under given constraints, several new exact solutions were obtained and illustrated through 3D, 2D, and contour plots using modern computational tools. A planar dynamical system is derived from the proposed model to perform a sensitivity analysis concerning initial conditions. This approach allows for a detailed examination of how slight changes in initial values can affect the system's evolution and long-term dynamics. The results indicate that wave singularities can be effectively controlled by varying the wave velocity. The method led to the discovery of novel solitary wave structures, including soliton types not previously found in the literature. Overall, the study confirms the robustness and applicability of the proposed analytical approach for addressing a wide range of non-linear partial differential equations arising in physical and engineering contexts.

Acknowledgments. Funding: No funding was available for this research.
Consent for publication: Not applicable.
Consent to participate and Ethics approval: Not applicable.
Availability of data and material: No data sets were collected or analysed during this study, there is no applicable data sharing for this paper.
Competing interests: The authors confirm that they do not have any competing interests.

REFERENCES

[1] S. Abbagari, A. Houwe, L. Akinyemi, Y. Saliou, & T. B. Bouetou, *Modulation instability gain and discrete soliton interaction in gyrotropic molecular chain*, Chaos, Solitons & Fractals, **160**, (2022) 112255.

[2] Z. Abbas, & N. Mushahid, *Soliton solutions of coupled complex modified Korteweg-de Vries system through Binary Darboux transformation*, Punjab Univ. J. Math., **53**, No. 10 (2021).

[3] T. Abdulkadir Sulaiman, & A. Yusuf, *Dynamics of lump-periodic and breather waves solutions with variable coefficients in liquid with gas bubbles*, Waves in Random and Complex Media, (2021) 1-14.

[4] H.Ahmad, M. N. Alam, & M. Omri, *New computational results for a prototype of an excitable system*, Results in Physics, **28**, (2021) 104666.

[5] H. Ahmad, T. A. Khan, P. S. Stanimirovic, W. Shatanawi, & T. Botmart, *New approach on conventional solutions to nonlinear partial differential equations describing physical phenomena*, Results in Physics, **41**, (2022) 105936.

[6] L. Akinyemi, H. Rezazadeh, S. W. Yao, M. A. Akbar, M. M. Khater, A. Jhangeer, & H. Ahmad, *Nonlinear dispersion in parabolic law medium and its optical solitons*, Results in Physics, **26**, (2021) 104411.

[7] G. Akram, M. Sadaf, & M. A. U. Khan, *Soliton solutions of the resonant nonlinear Schrödinger equation using modified auxiliary equation method with three different nonlinearities*, Mathematics and Computers in Simulation, **206**, (2023) 1-20.

[8] M. Alabedalhadi, *Exact travelling wave solutions for nonlinear system of spatiotemporal fractional quantum mechanics equations*, Alexandria Engineering Journal, **61**, No. 2 (2022) 1033-1044.

[9] M. N. Alam, I. Talib, O. Bazighifan, D. N. Chalishajar, & B. Almarri, *An analytical technique implemented in the fractional Clannish Random Walker's Parabolic equation with nonlinear physical phenomena* Mathematics, **9**, No. 8 (2021) 801.

[10] M. N. Alam, O. A. İlhan, M. S. Uddin, & M. A. Rahim, *Regarding on the Results for the Fractional Clannish Random Walker's Parabolic Equation and the Nonlinear Fractional Cahn-Allen Equation*, Advances in Mathematical Physics, **2022** No 1, (2022) 5635514.

[11] K. K. Ali, A. M. Wazwaz, & M. S. Osman, *Optical soliton solutions to the generalized nonautonomous nonlinear Schrödinger equations in optical fibers via the sine-Gordon expansion method*, Optik, **208**, (2020) 164132.

[12] K. K. Ali, A. Yokus, A. R. Seadawy, & R. Yilmazer, *The ion sound and Langmuir waves dynamical system via computational modified generalized exponential rational function*, Chaos, Solitons & Fractals, **161**, (2022) 112381.

[13] A. Atangana, & J.F. Gómez-Aguilar, *Numerical approximation of Riemann Liouville definition of fractional derivative: from Riemann Liouville to Atangana Baleanu*, Numerical Methods for Partial Differential Equations, **34**, No. 5 (2018) 1502-1523.

[14] D. Baleanu, K. Diethelm, E. Scalas, & J.J Trujillo, *Fractional calculus: models and numerical methods* (Vol. 3). World Scientific, (2016).

[15] O. A. Bruzzone, D. V. Perri, & M. H. Easdale, *Vegetation responses to variations in climate: A combined ordinary differential equation and sequential Monte Carlo estimation approach. Ecological Informatics*, (2022) 101913.

[16] M. R. A. Fahim, P. R. Kundu, M. E.Islam, M. A. Akbar & M. S. Osman, *Wave profile analysis of a couple of (3+ 1)-dimensional nonlinear evolution equations by sine-Gordon expansion approach*, Journal of Ocean Engineering and Science, **7**, No. 3 (2022) 272-279.

[17] B. Ghanbari & J.F. Gómez-Aguilar, *New exact optical soliton solutions for nonlinear Schrödinger equation with second-order spatio-Temporal dispersion involving M-derivative*, Modern Physics Letters B, **33**, No. 20 (2019) 1950235.

[18] B. Ghanbari, & J. F. Gómez-Aguilar, *The generalized exponential rational function method for Radhakrishnan-Kundu-Lakshmanan equation with $\mathfrak{B}$-conformable time derivative*, Revista mexicana de fÃsica, **65**, No. 5 (2019) 503-518.

[19] O. Guner, A. Bekir, & O. Ünsal, *Two reliable methods for solving the time fractional Clannish Random Walker's Parabolic equation*, Optik, **127**, No. 20 (2016) 9571-9577.

[20] R, Hirota,*Exact Solutions of the Korteweg-de Vries Equation for Multiple Collisions of Solitons*, Physical Review Letters, **27**, (1971) 1192-1194.

[21] H. U. Jan, I. A. Shah, N. U. Tamheeda, & A. Ullah, *Approximation of Nonlinear Sine-Gordon Equation via RBF-FD Meshless Approach*, Punjab Univ. J. Math., **55**, No. 9 (2023) 357-370. K.Hosseini, M. Mirzazadeh, M. Ilie, & S. Radmehr, *Dynamics of optical solitons in the perturbed Gerdjikov–Ivanov equation*, Optik, **206**, (2020) 164350.

[22] B. Karaman, *The use of improved-F expansion method for the time-fractional Benjamin–Ono equation*, Revista de la Real Academia de Ciencias Exactas, Físicas y Naturales. Serie A. Matemáticas, **115**, No. 3 (2021) 1-7.

[23] R. Khalil, M. Al Horani, A. Yousef, & M. Sababheh, *A new definition of fractional derivative*, Journal of computational and applied mathematics, **264**, (2014) 65-70.

[24] M. Khater, A. Jhangeer, H. Rezazadeh, L. Akinyemi, M. A. Akbar, M. Inc & H. Ahmad, *New kinds of analytical solitary wave solutions for ionic currents on microtubules equation via two different techniques*, Optical and Quantum Electronics, **53** No. 11 (2021) 1-27.

[25] F. S. Khodadad, S. M. Mirhosseini-Alizamini, B. Günay, L. Akinyemi, H. Rezazadeh, & M. Inc, *Abundant optical solitons to the Sasa-Satsuma higher-order nonlinear Schrödinger equation*, Optical and Quantum Electronics, **53**, No. 12 (2021) 1-17.

[26] Z. Li, X. Xie, & C. Jin, *Phase portraits and optical soliton solutions of coupled nonlinear Maccari systems describing the motion of solitary waves in fluid flow*, Results in Physics, **41**, (2022) 105932.

[27] S. Z. Majid, W. A. Faridi, M. I. Asjad, M. Abd El-Rahman, & S. M. Eldin, *Explicit Soliton Structure Formation for the Riemann Wave Equation and a Sensitive Demonstration*, Fractal and Fractional, **7**, No. 2 (2023) 102.

[28] M. S. Osman, H. Almusawa, K. U. Tariq, S. Anwar, S. Kumar, M. Younis, & W. X. Ma, *On global behavior for complex soliton solutions of the perturbed nonlinear Schrödinger equation in nonlinear optical fibers*, Journal of Ocean Engineering and Science, **7**, No 5 (2022) 431-443.

[29] N. Raza, Z. Hassan, & J. F. Gómez-Aguilar, *Extraction of new super-Gaussian solitons via collective variables*, Optical and Quantum Electronics, **53**, (2021) 1-15.

[30] W. Razzaq, A. Zafar, H. M. Ahmed, & W. B. Rabied, *Construction solitons for fractional nonlinear Schrodinger equation with ß-time derivative by new sub-equation method*, Journal of Ocean Engineering and Science, 2022.

[31] S. T. Rizvi, A. R. Seadawy, S. Ahmed, & K. Ali, *Einstein's vacuum field equation: lumps, manifold periodic, generalized breathers, interactions and rogue wave solutions*, Optical and Quantum Electronics, **55**, No. 2 (2023) 1-25.

[32] S. T. Rizvi, A. R. Seadawy, S. K. Naqvi, S. O. & Abbas, *Study of mixed derivative nonlinear Schrödinger equation for rogue and lump waves, breathers and their interaction solutions with Kerr law*, Optical and Quantum Electronics, **55**, No. 2 (2023) 177.

[33] A. R. Seadawy, A. Ali, & M. H. Raddadi, *Exact and solitary wave solutions of conformable time fractional Clannish Random Walker's Parabolic and Ablowitz-Kaup-Newell-Segur equations via modified mathematical methods*, Results in Physics, **26**, (2021) 104374.

[34] Y. Shen, B. Tian, & X. T. Gao, *Bilinear auto-Bäcklund transformation, soliton and periodic-wave solutions for a (2+1)-dimensional generalized Kadomtsev–Petviashvili system in fluid mechanics and plasma physics*, Chinese Journal of Physics, **77**, (2022) 2698-2706.

[35] A. Sivaporn, S. Surattana, & K. Sanoe, *New exact solutions for the time fractional clannish random Walkerls parabolic equation by the improved tan* $(\phi-(\zeta)/2)$*-expansion method*, AMM, Chiang Mai University, Chiang Mai, Thailand, (2017).

[36] J. V. D. C. Sousa, & E. C. de Oliveira, *A new truncated* M*-fractional derivative type unifying some fractional derivative types with classical properties*, arXiv preprint arXiv, (2017) 1704.08187.

[37] S. F. Tian, M. J. Xu, T. T. & Zhang, *A symmetry-preserving difference scheme and analytical solutions of a generalized higher-order beam equation*, Proceedings of the Royal Society A, **477**, No. 2255 (2021) 20210455.

[38] N. Ullah, M. I. Asjad, J. Awrejcewicz, T. Muhammad, & D. Baleanu, *On soliton solutions of fractional-order nonlinear model appears in physical sciences*, AIMS Mathematics, **7**, No. 5 (2022) 7421-7440. doi: 10.3934/math.2022415

[39] N. Ullah, H. U. Rehman, M. I. Asjad, H. Ashraf, & A. Taskeen, *Dynamic study of Clannish Random Walker's parabolic equation via extended direct algebraic method*, Optical and Quantum Electronics, **56** No. 2, (2024) 183.

[40] S. W. Yao, R. Manzoor, A. Zafar, M. Inc, S. Abbagari, & A. Houwe, *Exact soliton solutions to the Cahn–Allen equation and Predator–Prey model with truncated M-fractional derivative*, Results in Physics, **37** (2022) 105455.

[41] A. Zafar, M. Shakeel, A. Ali, L. Akinyemi, & H. Rezazadeh, *Optical solitons of nonlinear complex Ginzburg–Landau equation via two modified expansion schemes*, Optical and Quantum Electronics, **54**, (2022) 1-15.

[42] E.M. Zayed, K.A. Gepreel, R.M. Shohib, M.E. Alngar & Y. Yıldırım, *Optical solitons for the perturbed Biswas-Milovic equation with Kudryashov's law of refractive index by the unified auxiliary equation method*, Optik, **230**, (2021) 166286.

[43] R. Zhang, S. Bilige, & T. Chaolu, *Fractal solitons, arbitrary function solutions, exact periodic wave and breathers for a nonlinear partial differential equation by using bilinear neural network method*, Journal of Systems Science and Complexity, **34**, No. 1 (2021) 122-139.

[44] T. Y. Zhou, B. Tian, C. R. Zhang, & S. H. Liu, *Auto-Bäcklund transformations, bilinear forms, multiple-soliton, quasi-soliton and hybrid solutions of a (3+1)-dimensional modified Korteweg-de Vries-Zakharov-Kuznetsov equation in an electron-positron plasma*, The European Physical Journal Plus, **137**, No. 8 (2022) 1-17.